

UAV-Assisted Real-Time Disaster Detection Using Optimized Transformer Model

Branislava Jankovic, Sabina Jangirova, Waseem Ullah, Latif U. Khan, Mohsen Guizani
[branislava.jankovic@mbzuai.ac.ae, sabina.jangirova@mbzuai.ac.ae, waseemullah@ieee.org,
latif.u.khan2@gmail.com, mguizani@ieee.org]

Mohamed Bin Zayed University of Artificial Intelligence, United Arab Emirates.

Abstract—Disaster recovery and management present significant challenges, particularly in unstable environments and hard-to-reach terrains. These difficulties can be overcome by employing unmanned aerial vehicles (UAVs) equipped with onboard embedded platforms and camera sensors. In this work, we address the critical need for accurate and timely disaster detection by enabling onboard aerial imagery processing and avoiding connectivity, privacy, and latency issues despite the challenges posed by limited onboard hardware resources. We propose a UAV-assisted edge framework for real-time disaster management, leveraging our proposed model optimized for real-time aerial image classification. The optimization of the model employs post-training quantization techniques. For real-world disaster scenarios, we introduce a novel dataset, DisasterEye, featuring UAV-captured disaster scenes as well as ground-level images taken by individuals on-site. Experimental results demonstrate the effectiveness of our model, achieving high accuracy with reduced inference latency and memory usage on resource-constrained devices. The framework’s scalability and adaptability make it a robust solution for real-time disaster detection on resource-limited UAV platforms.

Index Terms—Remote Sensing, Unmanned Aerial Vehicles, Edge Inference, Image Classification, Optimization, Resource-Constrained Devices, Real-Time.

I. INTRODUCTION

OVER many decades, humanity and forests have faced various disasters that have claimed countless lives and inflicted significant financial losses. These events affect both economically developed and underdeveloped regions, underscoring the persistent limitations of current technological solutions in effectively mitigating disaster impacts. The United Arab Emirates registered a record-breaking rainfall, reaching 254.8mm in less than 24 hours [6] in 2024, resulting in five deaths, the cancellation of 1,244 flights, and the suspension of routes between emirates. It is estimated that around 544.6 million dollars of funds were assigned to deal with damage caused by the flood. At the same time, experts emphasized that European countries must step up forest management after a massive increase in forest fires in the Balkans during the last few years [7]. Forest management, or disaster management in general, involves a range of actions designed to minimize the impact of disasters on society and the environment. Early detection of disaster nodes can help reduce their harmful causes and eliminate them more efficiently. On the other hand, an adequate ongoing response and effective remediation of the consequences can prevent the disruption of the population’s

normal rhythm. Due to uncertain outcomes and hard-to-reach terrains, the adoption of UAVs and UAV-based models for detection, observation, and studying passive and active threats and risks at incident scenes could significantly reduce the need for human intervention as well as human error [8].

UAVs have the capability to access locations that are difficult or dangerous for humans to reach. When equipped with camera sensors, they enable the real-time capture and transfer of high-resolution images. Traditionally, these images are processed using cloud computing frameworks; however, this approach faces significant challenges, including high latency, limited throughput, increased power consumption, and dependency on reliable cloud services, which may not always be available in disaster-prone or remote areas. Therefore, onboard processing is required at the edge. However, UAVs come with limited computational resources and low-power constraints, which can be challenging in performing computer vision tasks due to massive neural network models [9]. Existing solutions for disaster management on UAVs hardly rely on shallow networks or compressed CNN models [9], [2], [3], [4], [8]. The disadvantage of shallow networks is their insufficient complexity, which limits learning valuable features for classification. On the other hand, CNNs struggle with larger receptive fields. Consequently, more complex architectures, such as transformers, need to be considered. This work addresses the problem of onboard disaster classification for UAVs using complex neural networks. We present a UAV-assisted edge framework that trains a transformer-based neural network on different aerial image databases, which is further optimized to provide the best exchange between accuracy and performance and operate on edge devices. Moreover, we tackle the lack of real-world relevance in existing datasets, which mainly focus on certain disaster cases or contain only a few disaster cases, making them unsuitable for real-world adaptation. We construct a novel database with seven distinguishing disaster cases featuring UAV-captured scenes as well as ground-level images taken by individuals on-site.

These are the summarized main contributions of this work:

- 1) We introduce a UAV-assisted edge framework for disaster management, leveraging an optimized transformer-based architecture for accurate aerial image classification. Our framework is tested on existing aerial imagery datasets. Additionally, we explore various compression and quanti-

zation techniques, providing an in-depth analysis of their impacts on performance.

- 2) To enhance relevance and realism, we construct a novel dataset DisasterEye, containing real-world scenes captured by UAVs and individuals on-site.
- 3) Our Proposed model achieved real-time performance, $3x$ to $5x$ times faster than the original, with almost similar accuracy. Moreover, we validate results on a resource-constrained device to determine the potential for deploying our solution on UAVs.

The rest of this paper is structured as follows: Section II provides related works and background. Section III explains the methodology, in particular, training and optimization of the model. In Section IV, we analyze datasets and results. Finally, Section V provides concluding remarks and discusses directions for future work.

II. BACKGROUND AND RELATED WORK

This section discusses previous works on disaster classification with UAVs and highlights the background knowledge of Vision Transformers and Optimization techniques.

Authors in [15] proposed a vision sensor-based fire detection method for an early-warning fire-monitoring system with an SVM classifier. On the other hand, [16], [19] used a VGG16-based neural network for fire classification. At the same time, [17], [14] used residual-based neural networks. Shallow architectures specially tailored for fire detection were introduced in [20], [36], [5], [3], [4], [10], [9], [2], [11], focused on classification of disaster aerial images. Authors in [12] presented a new high-resolution aerial imagery dataset for post-flood scene understanding, FloodNet, further used in [13] for semisupervised classification and supervised semantic segmentation. In [18], researchers tackled the problem of low-altitude imagery and used semisupervised training techniques to learn from noisy, constrained, and erroneous labels, while works presented in [21], [8] studied the issue of model size.

Most previous solutions rely on lightweight convolutional neural networks. CNNs may be easily exported on edge devices but are also limited by the number of learning parameters, which makes them unable to capture the valuable features [41].

Vision Transformers

Based on attention mechanisms, Transformers were initially designed for sequence modeling and transduction tasks [22]. The ability to effectively capture long-range dependencies guided researchers to utilize them for computer vision tasks. Vision Transformer (ViTs) [23] is the first transformer-based architecture that was applied to the computer vision domain. Thanks to the use of attention mechanisms to capture global receptive fields, they quickly showed effectiveness on computer vision tasks, as classification [23], object detection [25], semantic segmentation [24] and many more. Nevertheless, the significant number of parameters and computational overhead of transformers introduce a challenge during deployment to

resource-constrained hardware devices [26]. Thus, the compression approaches for ViTs are necessary for practical deployments [27].

Optimization Techniques

Most existing Post-Training Quantization approaches have been developed and tested on CNNs. Nevertheless, they lack appropriate handling of transformer-based models with non-linear arithmetic, such as Softmax, GELU, and LayerNorm. FasterTransformer [28] leaves the nonlinear operations as dequantized floating-point arithmetic. Other solutions are Rank-ing loss [29], presented to maintain the correct relative order of the quantized attention map, Q-ViT [34] that takes the quantization bit-widths and scales as learnable parameters, PTQ4ViT [30] with twin uniform quantization and a Hessian metric for evaluation of different scaling factors. Moreover, FQ-ViT [26] introduces two different quantizations specially tailored for LayerNorm and Softmax. However, since it is based on I-BERT [35], it ignores the GELU operation, which causes mixed-precision inference. RepQ-ViT [33] addresses the extreme distributions of LayerNorm and Softmax activations, while PSAQ-ViT [31], [32] pushes the quantization of ViTs to data-free scenarios based on patch similarity.

III. METHODOLOGY

A. Problem Formulation

While traditional CNNs have been widely used in UAV disaster classification tasks because of their effectiveness on edge devices, they rely on localized receptive fields, which can affect the capture of long-range dependencies essential for complex scene understanding. In contrast, Vision Transformers surpassed this limitation by introducing attention mechanisms [23]. Nevertheless, deployment on edge devices becomes a challenge due to their vast number of parameters and higher computational costs. Our proposed framework builds on these insights by optimizing a transformer-based model specifically for UAV disaster classification tasks, employing PTQ methods to meet the field's real-time, low-power demands of UAV-assisted edge frameworks.

The main steps of developing the pipeline for the classification of disasters are divided into two stages 1: the **Model Training Stage** including preprocessing and training of the model, and the **Model Inferencing Stage** incorporating optimization of the network and evaluation on inference.

B. Model Architecture

We utilize the Swin transformer [25] for disaster classification. Its hierarchical architecture with shifting windows allows performance at various scales with linear computational complexity. This enables the model to focus on detailed and global features, which is impossible with CNNs. In the beginning, a patch-splitting module splits RGB images into non-overlapping patches. Each patch represents a "token" that will be further projected into an arbitrary dimension with a linear embedding layer. To produce a hierarchical architecture, patch merging

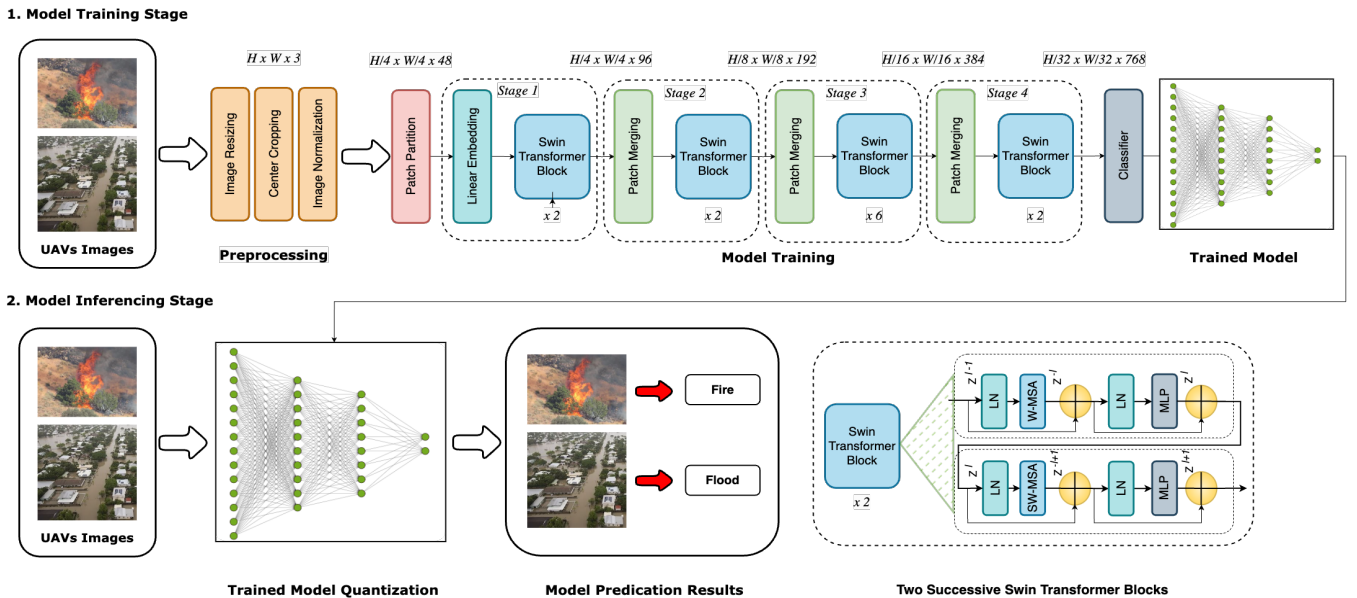


Fig. 1: Overview of the proposed framework: 1) Model training, where UAV-captured images are processed through preprocessing, feature extraction using a backbone transformer model, and training; and 2) Model inference, enabling real-time disaster detection.

layers reduce the number of "tokens" as the network gets deeper. At the same time, the number of channels increases. Swin Transformer blocks follow the linear embedding layer in the first stage and patch merging layers in the other stages. Their role is to transform features while keeping the same resolution. Figure 1 represents two successive Swin transformer blocks. In the second block, the standard multi-head self-attention (W-MSA) module is replaced by a module based on shifted windows, while the rest of the layers remain the same. This was done due to a lack of connections between neighboring non-overlapping windows.

C. Model Optimization

In this work, we use Post-Training Quantization to optimize our models. PTQ is a technique for lowering computational and memory expenses of running inference. This is done by defining the weights, activations, and attention with low-precision data types such as 16-bit floating point and integer instead of the original 32-bit floating point. The model can achieve faster performance thanks to simpler matrix multiplications by reducing the number of bits. Moreover, it requires less storage memory and consumes less energy. In this work, we are employing the TensorRT quantization technique and compare it with MinMax, EMA [37], Percentile [38], OMSE [39], and FQ-Vit [26], quantization methods. TensorRT is an SDK developed by NVIDIA specifically for faster performance on NVIDIA GPUs [40], using five different optimizations: precision calibration, layer, and tensor fusion, kernel auto-tuning, multi-stream executions, and dynamic tensor memory.

D. Model Inference

We comprehensively evaluate the inference of the optimized model across two distinct platforms, one of which is resource-

constrained. Each platform provides unique hardware capabilities that impact inference speed, memory consumption, and overall efficiency, allowing us to assess the adaptability and scalability of our model across different environments.

IV. EXPERIMENTAL RESULTS

A. Datasets

Our work utilizes three different datasets: DFAN [36], AIDER [10], and DisasterEye, our custom dataset. Figure 2 shows example images in these datasets.



Fig. 2: Samples images of various UAVs based datasets: a) DFAN; b) AIDER; c) DisasterEye.

The DFAN dataset is a medium-scale database of 3,803 images representing different fire scenarios, divided into 12 imbalanced classes. The photos were sourced from multiple locations, including videos, leading to duplicate images. Due to noisiness and huge class diversity, this dataset hinders the training of models. The AIDER dataset [10] is a unique and comprehensive resource for disaster classification tasks. It comprises 6923 images divided into five classes, including

four disaster classes: collapsed buildings, fire, flood, and traffic accidents, followed by a normal class. Aerial disaster images were manually collected from various online sources. Each disaster class contains approximately 500 photographs, while the average class has a significantly more extensive set of 4,390 images, which can challenge models on inference.

Previous datasets contain only a few disaster cases or focused on only one disaster case, such as fire. Therefore, the models trained on these databases are unsuitable for real-world applications. Consequently, a benchmark dataset that will resemble real-life scenarios is needed. DisasterEye is our custom dataset containing images taken with UAVs during or after disasters, as well as images taken from individuals on sight. This dataset consists of 2751 images separated into eight classes: flood, fire, traffic accident, post-earthquake, mudslide, landslide, normal, and conflict. The samples are collected from various sources such as Google Images and YouTube. Figure 3 shows the distribution of instances per class in training, validation, and testing subsets.

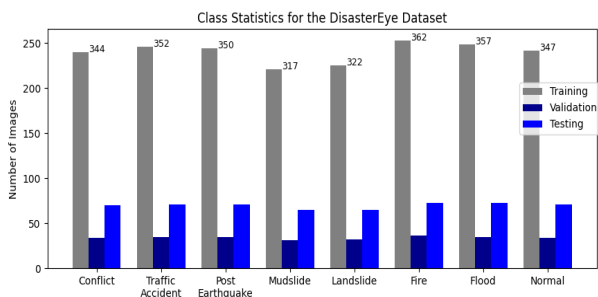


Fig. 3: Class statistics for the DisasterEye dataset.

B. Evaluation Metrics

We used the same evaluation metrics—accuracy, precision, recall, and F1-score for a fair assessment of the proposed model, evaluating its performance in disaster detection on UAVs and under various quantization strategies. The accuracy expresses the number of correctly classified instances in one dataset, while loss is used to analyze the performance of trained models. The f1-score provides a balance between precision-positive predictive value and recall-model sensitivity. Apart from the mentioned metrics, we focus on latency, throughput, and model size to evaluate quantization strategies. Latency presents the model’s time to complete a single inference. Throughput tells us how many instances can be processed in a specific time frame. Finally, model size is essential for deploying the models on edge devices.

C. Training Performance

Before training, each dataset’s images are divided into training, validation, and testing subsets. Splitting the data is followed by image preprocessing, including resizing, cropping, and normalization to ensure consistency in size, format, and intensity distribution. We fine-tune the transformer-based network trained on ImageNet with our datasets to avoid overfitting

and achieve good generalization. All models are fine-tuned until convergence with the Adam optimizer and a learning rate of $1e - 5$. The training is conducted on a desktop computer with an NVIDIA GeForce RTX 2080 12 GB, an Intel Xeon Silver 4215 CPU running at 2.50 GHz, and 12 GB of RAM. We evaluate our proposed model on three different datasets: AIDER, DFAN, and DisasterEye, using categorical cross-entropy loss. Our model performs satisfactorily on the AIDER dataset, while a larger number of classes and a limited number of instances in DFAN and DisasterEye hinder the model’s generalization II.

D. Optimization Performance

TensorRT allows two types of precision calibration: FP16 and INT8. Precision calibration with 16-bit reduces the memory footprint, which minimizes the Model Size roughly by half and gives four times faster inference. However, this solution can affect the models’ accuracy. This can be seen from the performance of the quantized model on the DFAN dataset II. The accuracy of the model dropped by roughly 1.9%. We use plain INT8 quantization in TensorRT with default dynamic ranges to optimize our model to INT8 precision. We do not observe a notable drop in accuracy (more than 0.3%) compared to FP16 quantization on our datasets. However, there is a significant drop in model size, which is now reduced by roughly 70%. At the same time, latency is slightly increased compared with TensorRT FP16 optimization due to the need for precision scaling and zero-point adjustments. Overall, both FP16 and INT8 quantization with TensorRT achieve real-time performance II.

E. Visual Results Analysis

Figure 4 shows the visual results of the performance of our quantized model on our datasets. Usually, the model mistakes similar classes, such as landslide and mudslide, as seen from the last example in the third row. Moreover, the model produces mistakes due to its tendency to associate specific objects or features with particular classes. For example, the last picture in the first row shows scenery that can be associated with collapsed buildings. Finally, we observe failure cases when more than one disaster is illustrated in the photo. The last picture in the second row shows a bus fire, but cars are also present.

Increasing the number of frames for each category could potentially solve the problems mentioned above. Moreover, introducing multilabel classification per frame might reduce some of the issues.

F. Ablation Experiments

In this section, we evaluate the performance of our model while employing different optimization techniques. Apart from the proposed TensorRT optimization, we use MinMax, EMA, OMSE, Percentile, and FQ-ViT quantization techniques. Results can be found in Table II. MinMax, EMA, OMSE, and Percentile optimization techniques were designed mainly for

TABLE I: Summary of results of previous models trained on our datasets and our compressed, proposed model.

Dataset	Models	System specification	F1-Score	FPS	Number of Parameters [M]	Model Size [MB]	
AIDER	EmergencyNet [9]	ARM Cortex-A57	0.957	25	0.09	0.78	
	TinyEmergencyNet [2]	NVIDIA Quadro RTX 5000 GPU	0.940	-	0.04	0.15	
	MFEMANet [1]	-	0.970	-	-	-	
	MobileNet [8]	Jetson Nano	0.980	4	3.2	37.00	
	MobileNet Compressed [8]	Jetson Nano	-	71	3.2	7.00	
	Our Model FP16	NVIDIA T4 GPU 16 GB GPU	0.980	336.92	27.5	58.89	
	Our Model INT8	NVIDIA T4 GPU 16 GB GPU	0.977	236.41	27.5	36.76	
	Our Model INT8	Jetson Nano	0.977	45.22	27.5	34.00	
DFAN	DFAN [36]	NVIDIA GPU 2070 12 GB GPU	0.870	70.55	23.9	83.63	
	DFAN Compressed [36]	NVIDIA GPU 2070 12 GB GPU	0.860	125.33	23.9	41.09	
	MobileNet [36]	NVIDIA GPU 2070 12 GB GPU	0.810	-	3.2	37.00	
	MAFire-Net [5]	NVIDIA GeForce RTX-3090 GPU	0.875	78.31	-	74.43	
	ADFireNet [3]	NVIDIA GeForce RTX-3090 GPU	0.900	72.50	7.2	38.00	
	MobileNetV3+MSAM [4]	NVIDIA GeForce RTX-3090 GPU	0.906	75.15	3.2	25.20	
	Our Model FP16	NVIDIA T4 GPU 16 GB GPU	0.912	305.43	27.5	58.85	
	Our Model INT8	NVIDIA T4 GPU 16 GB GPU	0.910	240.17	27.5	34.91	
		Our Model INT8	Jetson Nano	0.910	45.04	27.5	34.00

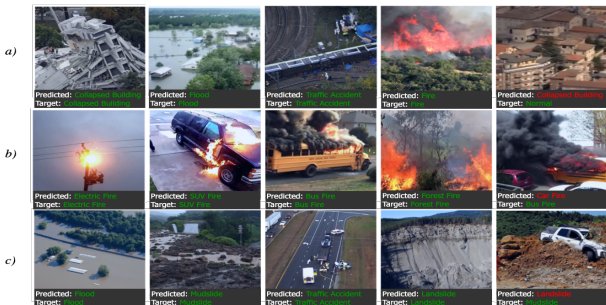


Fig. 4: Visual Results of the proposed model on benchmark datasets: a) AIDER, b) DFAN, and c) DisasterEye.

CNN architectures. Therefore, they focus on Convolutional, Linear, and MatMul modules while lacking solutions for handling Softmax, LayerNorm, and GELU layers. This means many layers stay in a 32-bit floating point, resulting in the mix-precision network and unchanged model size; however, a significant speedup, enough for real-time performance, can be seen for all these methods. FQ-ViT, specially tailored for transformer-based architectures, introduces powers-of-two scale quantization and log-int quantization for LayerNorm and Softmax, respectively. However, FQ-ViT does not focus on GELU layers, leading to partial performance. Due to dequantized floating-point parameters during inference, efficient low-precision arithmetic units are not fully utilized, and, therefore, we get unsatisfactory model acceleration.

G. Comparison With the State-of-the-Art

Table I shows the performances of state-of-the-art models and our proposed method. Our model outperforms almost all previously trained networks in terms of f1-score on the AIDER dataset. In [8], authors used class weights due to unbalanced data to train MobileNet, while our results purely rely on transformers' capability to capture valuable information from frames. The limited network, such as MobileNet, performs poorly when trained on the DFAN dataset, which contains few samples and many classes. At the same time, our model

TABLE II: Optimization methods used on the proposed model.

Dataset	Method (w/a/att)	Accuracy	Latency [ms]	FPS	Model Size [MB]	
AIDER	Original 32/32/32	0.9825	48.87	20.46	107	
	MinMax 8/8/8	0.9789	37.01	27.02	107	
	EMA 8/8/8	0.9825	37.51	26.66	107	
	OMSE 8/8/8	0.9825	37.62	26.58	107	
	Percentile 8/8/8	0.9818	37.34	26.78	107	
	FQ-ViT 8/8/4	0.9839	55.90	17.89	107	
	TensorRT INT8	0.9770	4.23	236.41	36.76	
	TensorRT FP16	0.9799	2.97	336.92	58.89	
	DFAN	Original 32/32/32	0.9309	63.36	15.78	107
		MinMax 8/8/8	0.9096	40.64	24.61	107
EMA 8/8/8		0.9016	40.16	24.90	107	
OMSE 8/8/8		0.9149	40.71	24.56	107	
Percentile 8/8/8		0.9149	39.69	25.20	107	
FQ-ViT 8/8/4		0.9149	59.63	16.77	107	
TensorRT INT8		0.9096	4.16	240.17	34.91	
TensorRT FP16		0.9122	3.27	305.43	58.85	
DisasterEye		Original 32/32/32	0.9016	79.54	12.57	107
		MinMax 8/8/8	0.8748	40.83	24.49	107
	EMA 8/8/8	0.8819	40.74	24.55	107	
	OMSE 8/8/8	0.9070	41.98	23.82	107	
	Percentile 8/8/8	0.8962	40.38	24.76	107	
	FQ-ViT 8/8/4	0.8855	59.70	16.75	107	
	TensorRT INT8	0.8945	4.33	230.73	33.47	
	TensorRT FP16	0.8962	3.01	332.26	58.74	

achieves the highest performance in terms of f1-score, outperforms other solutions [36], [5], [3], [4] on high computational GPU devices regarding speed and achieves real-time performance on resource-constrained devices. Consequently, our proposed framework's scalability and adaptability make it a valuable tool for deploying real-time disaster detection solutions on resource-limited UAV platforms.

V. CONCLUSION

This work confirms the effectiveness of transformer-based architectures for real-time disaster classification on UAVs. By utilizing advanced quantization techniques, the model substan-

tially reduces memory footprint and latency while maintaining accuracy across various disaster types. The results show that INT8 quantization with TensorRT significantly enhances model performance on edge devices, with minimal impact on accuracy for distinctive classes. The proposed framework demonstrates robust classification capabilities in diverse disaster scenarios and highlights the potential of deploying transformer models on UAVs for prompt and autonomous disaster response. Future work will focus on extending the framework with additional disaster scenarios and expanding the DisasterEye dataset.

REFERENCES

- [1] P. Bhadra, A. Balabantaray, and A. K. Pasayat, "MFEMANet: an effective disaster image classification approach for practical risk assessment," *Machine Vision and Applications*, vol. 34, p. 76, 2023. DOI: 10.1007/s00138-023-01430-1.
- [2] O. M. Mogaka, R. Zewail, K. Inoue, and M. S. Sayed, "TinyEmergencyNet: a hardware-friendly ultra-lightweight deep learning model for aerial scene image classification," *Journal of Real-Time Image Processing*, vol. 21, p. 51, 2024. DOI: 10.1007/s11554-024-01430-y.
- [3] H. Yar, X. Xu, J. Zhang, Z. Li, "An effective attention-based CNN model for fire detection in adverse weather conditions," *ISPRS Journal of Photogrammetry and Remote Sensing*, vol. 206, pp. 335–346, 2023. DOI: 10.1016/j.isprsjprs.2023.06.005.
- [4] H. Yar, Z. A. Khan, I. Rida, W. Ullah, M. J. Kim, and S. W. Baik, "An efficient deep learning architecture for effective fire detection in smart surveillance," *Image Vision Comput.*, vol. 145, no. C, pp. 104989, May 2024, doi: 10.1016/j.imavis.2024.104989.
- [5] T. Khan, Z. A. Khan, and C. Choi, "Enhancing real-time fire detection: an effective multi-attention network and a fire benchmark," *Neural Computing and Applications*, 2023. doi: <https://doi.org/10.1007/s00521-023-09298-y>.
- [6] *International Disaster Charter Activations by NASA*. Available at: <https://eol.jsc.nasa.gov/ESRS/Disasters/ShowIDCTracking.pl> (Accessed: Aug. 26, 2024).
- [7] *EFFIS - Statistics Portal*. Available at: <https://forest-fire.emergency.copernicus.eu/apps/effis.statistics/estimates> (Accessed: Aug. 26, 2024).
- [8] Ijaz, H., Qureshi, W. S., Khokhar, M. I. and Iqbal, M. (2023) 'A UAV-assisted edge framework for real-time disaster management,' *IEEE Transactions on Geoscience and Remote Sensing*, 61, pp. 1–13. doi: 10.1109/TGRS.2023.3306151.
- [9] Kyrkou, C. and Theocharides, T. (2020) 'EmergencyNet: Efficient aerial image classification for drone-based emergency monitoring using atrous convolutional feature fusion,' *IEEE Journal of Selected Topics in Applied Earth Observations and Remote Sensing*, 13, pp. 1687–1699. doi: 10.1109/JSTARS.2020.2969809.
- [10] Kyrkou, C. (2020) 'AIDER (Aerial Image Dataset for Emergency Response Applications),' *Zenodo*. doi: 10.5281/zenodo.3888300.
- [11] Y. Li, R. Chen, Y. Zhang, and H. Li, "A CNN-GCN framework for multi-label aerial image scene classification," in *Proc. IEEE Int. Geosci. Remote Sens. Symp. (IGARSS)*, Sep. 2020, pp. 1353–1356.
- [12] M. Rahnemoonfar, T. Chowdhury, A. Sarkar, D. Varshney, M. Yari, and R. R. Murphy, "FloodNet: A high-resolution aerial imagery dataset for post-flood scene understanding," *IEEE Access*, vol. 9, pp. 89644–89654, 2021.
- [13] S. Khose, A. Tiwari, and A. Ghosh, "Semi-supervised classification and segmentation on high-resolution aerial images," 2021, *arXiv:2105.08655*.
- [14] H. Xiang, L. Chen, and W. Xu, "DRFNet: A lightweight and high accuracy network for resource-limited implementation," in *Proc. IEEE 12th Int. Conf. ASIC (ASICON)*, Oct. 2017, pp. 1086–1089.
- [15] B. C. Ko, K.-H. Cheong, and J.-Y. Nam, "Fire detection based on vision sensor and support vector machines," *Fire Saf. J.*, vol. 44, no. 3, pp. 322–329, Apr. 2009. Available: <https://www.sciencedirect.com/science/article/pii/S0379711208000957>
- [16] S. Kim, W. Lee, Y.-S. Park, H.-W. Lee, and Y.-T. Lee, "Forest fire monitoring system based on aerial image," in *Proc. 3rd Int. Conf. Inf. Commun. Technol. Disaster Manage. (ICT-DM)*, Dec. 2016, pp. 1–6.
- [17] J. Sharma, O.-C. Granmo, M. Goodwin, and J. T. Fidge, "Deep convolutional neural networks for fire detection in images," in *Engineering Applications of Neural Networks*, G. Boracchi, L. Iliadis, C. Jayne, and A. Likas, Eds. Cham, Switzerland: Springer, 2017, pp. 183–193.
- [18] M. Presa-Reyes, Y. Tao, S.-C. Chen, and M.-L. Shyu, "Deep learning with weak supervision for disaster scene description in low-altitude imagery," *IEEE Trans. Geosci. Remote Sens.*, vol. 60, 2022, Art. no. 4704510.
- [19] Y. Zhao, J. Ma, X. Li, and J. Zhang, "Saliency detection and deep learning-based wildfire identification in UAV imagery," *Sensors*, vol. 18, no. 3, p. 712, Feb. 2018.
- [20] A. Jadon, M. Omama, A. Varshney, M. S. Ansari, and R. Sharma, "FireNet: A specialized lightweight fire & smoke detection model for real-time IoT applications," 2019, *arXiv:1905.11922*.
- [21] N. Shoukry, F. Ehab, and M. A. Salem, "An improved deep learning model for early fire and smoke detection on edge vision unit," in *Proc. 10th Int. Conf. Intell. Comput. Inf. Syst. (ICICIS)*, Dec. 2021, pp. 66–73.
- [22] A. Vaswani, N. Shazeer, N. Parmar, J. Uszkoreit, L. Jones, A. N. Gomez, Ł. Kaiser, and I. Polosukhin, "Attention is all you need," in *Advances in Neural Information Processing Systems (NeurIPS)*, 2017, pp. 5998–6008.
- [23] A. Dosovitskiy, L. Beyer, A. Kolesnikov, D. Weissenborn, X. Zhai, T. Unterthiner, M. Dehghani, M. Minderer, G. Heigold, S. Gelly, et al., "An image is worth 16x16 words: Transformers for image recognition at scale," in *Proc. Int. Conf. Learning Representations (ICLR)*, 2020.
- [24] S. Zheng, J. Lu, H. Zhao, X. Zhu, Z. Luo, Y. Wang, Y. Fu, J. Feng, T. Xiang, and P. H. S. Torr, "Rethinking semantic segmentation from a sequence-to-sequence perspective with transformers," in *Proc. IEEE/CVF Conf. Computer Vision and Pattern Recognition (CVPR)*, 2021.
- [25] Z. Liu, Y. Lin, Y. Cao, H. Hu, Y. Wei, Z. Zhang, S. Lin, and B. Guo, "Swin transformer: Hierarchical vision transformer using shifted windows," *arXiv preprint arXiv:2103.14030*, 2021.
- [26] Y. Lin, T. Zhang, P. Sun, Z. Li, and S. Zhou, "FQ-ViT: Post-Training Quantization for Fully Quantized Vision Transformer," *arXiv preprint arXiv:2111.13824*, 2023. Available: <https://arxiv.org/abs/2111.13824>
- [27] Z. Li and Q. Gu, "I-ViT: Integer-only Quantization for Efficient Vision Transformer Inference," *arXiv preprint arXiv:2207.01405*, 2023. Available: <https://arxiv.org/abs/2207.01405>
- [28] NVIDIA, *FasterTransformer*, NVIDIA Corporation, 2022.
- [29] Z. Liu, Y. Wang, K. Han, W. Zhang, S. Ma, and W. Gao, "Post-training quantization for vision transformer," in *Advances in Neural Information Processing Systems*, vol. 34, 2021.
- [30] Z. Yuan, C. Xue, Y. Chen, Q. Wu, and G. Sun, "PTQ4ViT: Post-training quantization framework for vision transformers," *arXiv preprint arXiv:2111.12293*, 2021. Available: <https://arxiv.org/abs/2111.12293>
- [31] Z. Li, M. Chen, J. Xiao, and Q. Gu, "PSAQ-ViT v2: Towards accurate and general data-free quantization for vision transformers," *arXiv preprint arXiv:2209.05687*, 2022. Available: <https://arxiv.org/abs/2209.05687>
- [32] Z. Li, L. Ma, M. Chen, J. Xiao, and Q. Gu, "Patch similarity aware data-free quantization for vision transformers," in *European Conference on Computer Vision (ECCV)*, pp. 154–170, 2022.
- [33] Z. Li, J. Xiao, L. Yang, and Q. Gu, "RepQ-ViT: Scale reparameterization for post-training quantization of vision transformers," *arXiv preprint arXiv:2212.08254*, 2022. Available: <https://arxiv.org/abs/2212.08254>
- [34] Z. Li, T. Yang, P. Wang, and J. Cheng, "Q-ViT: Fully differentiable quantization for vision transformer," *arXiv preprint arXiv:2201.07703*, 2022. Available: <https://arxiv.org/abs/2201.07703>
- [35] S. Kim, A. Gholami, Z. Yao, M. W. Mahoney, and K. Keutzer, "I-BERT: Integer-only BERT quantization," in *Proc. Int. Conf. Machine Learning (ICML)*, PMLR, 2021, pp. 5506–5518.
- [36] Yar, H., Hussain, T., Agarwal, M., Khan, Z. A., Gupta, S. K., and Baik, S. W. (2022), "Optimized Dual Fire Attention Network and Medium-Scale Fire Classification Benchmark," *IEEE Transactions on Image Processing*, 31, pp. 6331–6343.
- [37] Jacob, B., Kligys, S., Chen, B., Zhu, M., Tang, M., Howard, A., Adam, H., and Kalenichenko, D. (2018) 'Quantization and training of neural networks for efficient integer-arithmetic-only inference,' *Proceedings of the IEEE Conference on Computer Vision and Pattern Recognition*, pp. 2704–2713.
- [38] Li, R., Wang, Y., Liang, F., Qin, H., Yan, J., and Fan, R. (2019) 'Fully quantized network for object detection,' *Proceedings of the IEEE/CVF Conference on Computer Vision and Pattern Recognition*, pp. 4270–4279.
- [39] Choukroun, Y., Kravchik, E., Yang, F., and Kisilev, P. (2019) 'Low-bit quantization of neural networks for efficient inference,' *IEEE/CVF International Conference on Computer Vision Workshops*. IEEE.
- [40] NVIDIA Corporation, "NVIDIA Developer," *NVIDIA Developer*, 2024. [Online]. Available: <https://developer.nvidia.com/>. [Accessed: Oct. 29, 2024].
- [41] V. Sze, Y. H. Chen, T. J. Yang, and J. S. Emer, "Efficient Processing of Deep Neural Networks: A Tutorial and Survey," *Proceedings of the IEEE*, vol. 105, no. 12, pp. 2295–2329, 2017. doi: 10.1109/JPROC.2017.2761740.